Laboratory Vibration Studies of Metro Tracks Equipped with Tuned Rail Dampers

Yingjie Wang[1, 2], Zuzana Dimitrovová[3, 4], and Jong-Dar Yau[5]

[1]School of Civil Engineering, Beijing Jiaotong University, Beijing, China
[2]Beijing Engineering and Technology Research Center of Rail Transit Line Safety and Disaster Prevention, Beijing, China.
[3]Department of Civil Engineering, NOVA School of Science and Technology, NOVA University of Lisbon, Lisbon, Portugal
[4]IDMEC, Instituto Superior Técnico, Universidade de Lisboa, Lisbon, Portugal
[5]Department of Civil Engineering, Tamkang University, New Taipei City, Taiwan

Abstract

With the rapid development of urban metro systems in the growing cities of China, a way to reduce metro-train induced track vibrations transmitted through ground to surrounding buildings has attracted the attention of engineering researchers. By using additional mass, damping and flexural stiffness to improve the dynamic performance of metro tracks, a Tuned Rail Damper (TRD) is developed to mitigate the vibrations of the metro-tracks. In this paper, a laboratory hammer test is designed and carried out to assess the vibration performance of a 3-interval (of 3x0.6m) metro track installed with the TRD sets. The hammer test results indicated that depending on the position of a hammer impulse acting on the 3-interval track unit, different excitation frequencies would be measured. Due to the flexural strengthening effect of the TRD, the composed TRD-track system has a robust ability to reduce vibrations and an increase of higher frequencies compared to conventional tracks, which can decrease the risk of clip failure in a fastening system subjected to intensive excitations from moving metro trains.

Keywords: Metro track, laboratory test, tuned rail damper, hammer test, frequency analysis

1. Introduction

To increase the transport capacity but reduce environmental impacts in the urbanization process of modern cities, underground transport infrastructure is often considered in newly developing cities of China during the past two decades for its advantages of mass transportation, energy savings and friendly environment. By the end of 2021, a total length of 7209.7 km of underground metro systems was in operation and 5093.1 km under construction [1]. For example, lengths of metro lines in operation in Shanghai and Beijing are 796.5 km and 680.0 km, respectively, which are the top two longest metro systems in the world[2]. During a long term operation, rail corrugations caused by repetitive wheel loadings of moving metro trains were observed in Beijing Metro Line 5 and Chongqing Metro Line 10, as demonstrated on photos of Fig. 1, which were related to perioral defects on the track surface.

(a) Beijing metro line 5[3] (b) Chongqing metro line 10[4]

Fig. 1. Photos of typical rail corrugations on metro track system

Due to the effects of periodic rail wear, rail corrugation may cause the following mechanical and environmental problems: abnormal vibrations on the track and vehicle components, contact cracks between the wheelset and bogie, broken clips of the fastening system, noise generation and micro soil vibration transmission[5-8]. In the past several decades, numerous railway researchers have studied the formation mechanisms of rail corrugation using theoretical and numerical models, experimental studies and field tests. However, due to the several components constituting the track structure and

the contact interaction between the wheelset and rail, the cause resulting in rail corrugation is a rather complicated issue. Till now, there is no well-established contact theory explaining the formation mechanism of rail corrugation phenomena[9-11]. Facing the abnormal vibrations of corrugated tracks, a Tuned Rail Damper (TRD) is developed to improve the dynamic performance on vibration suppression of the conventional metro-tracks. Maes et al. proposed a Double Tuned Rail Damper (DTRD) composed of a steel plate, an elastic layer, and a rubber mass, which showed a considerable attenuation of the envisaged pinned-pinned frequencies from the measurements at a SNCF (the Société Nationale des Chemins de Fer Français) test track[12]. Thompson et al. designed a TRD absorber system to increase the damping of the rail, and found it very promising with reductions of the track component of noise of around 6 dB from the laboratory and field tests[13]. Chen et al. evaluated the effects of TRD on the decay rate of the track through the laboratory tests, and the results indicated that the TRD can improve the dynamic characteristics of the Egg-III system track and DTVI-2 fastener track (a usual fastener type used in the metro-rail system of China)[14]. Jin et al. studied the influence of TRD on the decay rate of the rail with the egg fastening system based on the spectral element method and pointed out that adding the TRD weight and damping is beneficial in controlling rail vibration[15]. However, these papers mainly focus on the decay rate of the rail due to the TRDs.

As a dynamic absorber, the TRD is made of rubber materials and ductile iron, which can provide an additional mass, damping and flexural stiffness for the rail and further improve the dynamic performance against intensive vibrations caused by repetitive wheel loadings from moving metro cars. For verifications, a laboratory study on vibration reduction of metro tracks using the TRD developed herein will be presented in this paper. The full-scale experimental measurements of the metro track prototype were carried out in the “Laboratory of Rail Center (Rail-Lab)” of Beijing Jiaotong University (BJTU). Two main objectives are tackled by the present study: (1) to reveal the attenuation performance of the TRD on vibrations of metro tracks, and (2) to reveal the effect on the fastening system acting against clip failures from the dynamic response of the track equipped by the TRDs with the help of hammer tests.

2. Hammer Test Measurements

In railway engineering, hammer test measurements are widely employed to determine the dynamic behavior of the track or track components[16-19]. In this section, the hammer test measurements of the metro track with and without TRDs, performed in the laboratory Rail-Lab of BJTU are described. The field site of test tracks and corresponding components, instrumented devices and experimental plan for the dynamic measurements of metro tracks under hammer tests will be presented in Sections 2.1, 2.2 and 2.3, respectively.

2.1 Track Site

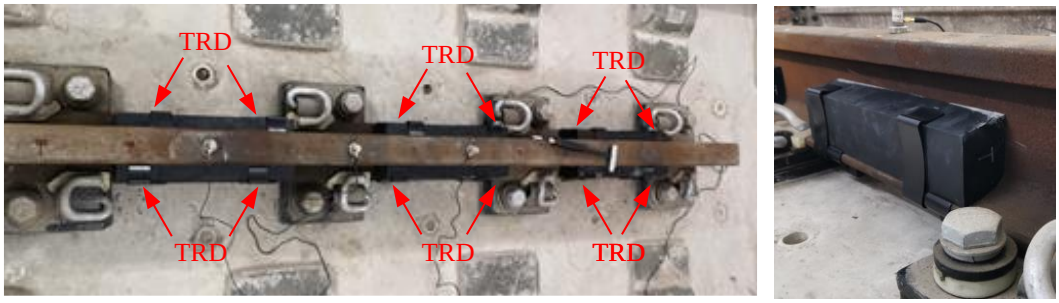

(a) With TRD

(b) Without TRD

Fig. 2 Prototype of metro track unit

The metro track site is located at Rail-Lab in BJTU and it contains a CHN60 rail fixed on the concrete base through the DTVI-2 fastener system, as shown in Fig. 2. The DTVI-2 fastener is commonly used on metro tracks in the sections without vibration reduction requirements in Beijing Metro System. Figure 2 shows a 3-interval short track supported by four DTVI-2 fasteners, as prepared for hammer tests in the laboratory. The tracks with or without TRD installed are shown in Fig. 2(a) and Fig. 2(b), respectively. According to the usual metro rail system, the mid-interval of two adjacent

sleepers of 0.6 m is selected, and the TRD blocks are mounted on both bottom flange sides of the rail. The material properties of the test rail are listed as follows: elastic modulus = 206 GPa, mass per length = 60.64 kg/m and Poisson's ratio = 0.3.

2.2 Setup of Experimental Instruments

In this study, the high frequencies of the track with or without TRD will be measured by a light hammer with hard tip test, which type will depend upon the selected frequency range of interest. Figure 3 shows an INV9312 hammer with a hard plastic tip, the weight of which is 210 grams and the test range of the impulse force is about 0-5000 N with a sensitivity of 1 mV/N. To capture the vibration response data of the test rail, a LC0159 accelerometer was placed on the top of the rail (see Fig. 4), and the measurement range of the sensor is up to 500 g with a sensitivity of 10 mV/g. In this test, the INV9312 hammer and LC0159 accelerometers were connected to the INV3062C data acquisition instrument, as shown in Fig. 5. Then the INV3062C was connected to one laptop through the internet cable for data transfer, as shown in Fig. 6. During the whole testing process, the INV3062C was controlled by the DASP-V11 software and the measured testing data were stored in the laptop for further spectral response analysis.

Fig. 3 INV9312 Hammer

Fig. 4 LC0159 accelerometer

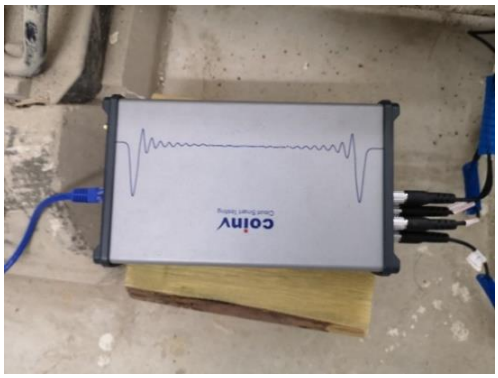

Fig. 5 INV3062C data acquisition instrument Fig. 6 Laptop

2.3 Experimental Plan of Hammer Tests

In this laboratory vibration test, a 2-meter rail is prepared, and three accelerometers called A1, A2 and A3 are used to measure the response of the test rail. Fig. 7 shows a schematic drawing of these accelerometers deployed on the test rail.

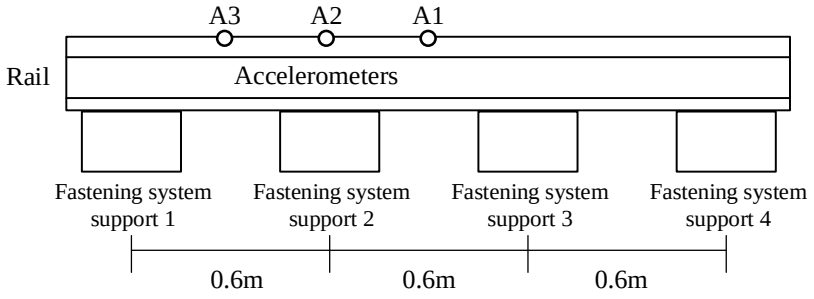

Fig. 7 A schematic drawing of the accelerometers' arrangement

All these accelerometers are placed on the top of the test rail, as indicated by the red circles marked in Figs. 8, 9 and 10. The accelerometers are divided into two groups, in Group 1, the accelerometers A1 and A3 are fixed at mid-span of the first two intervals (called mid-span section) of the test rail, as shown in Figs. 8 and 10, therefore,, the accelerometers A1 and A3 are also located at the middle of the TRD devices (see Figs. 8(a) and 10(a)). In Group 2 the single accelerometer A2 is mounted on the top of the supporting sleeper (called on-support section), as shown in Fig. 9. The test rails installed with and without the TRD are shown in Figs. 8, 9 and 10.

(a) With TRD (b) Without TRD

Fig. 8 Accelerometer A1

(a) With TRD (b) Without TRD

Fig. 9 Accelerometer A2

(a) With TRD (b) Without TRD

Fig. 10 Accelerometer A3

To capture the high frequencies of the track, the rail head was excited using a light hammer with hard tip, and the acceleration responses of the rail were measured at the locations of interest (see Fig. 7). Five excitation locations are shown schematically in Fig. 11, indicated from left to right, as F1, F2, F3, F4 and F5 respectively. Typically, the hammer impulse excitation is applied vertically, either on the rail of on-support section or the mid-span section. The hammer hit points F1, F3 and F5 are located at the mid-span of two adjacent sleepers, and F2 and F4 are on the top of the corresponding sleepers.

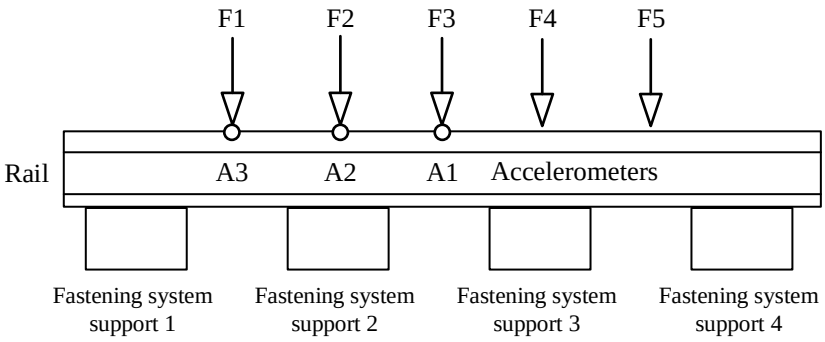

Fig. 11 Excitation locations

As an example, the hammer hit points on the on-support section and mid-span section are shown in Fig. 12. According to the accelerometers' arrangement, the hammer hit points F1, F2 and F3 are close to the accelerometers A3, A2 and A1.

(a) On-support section (b) Mid-span section

Fig. 12 Hammer impulse

3. Testing Results and Discussion

Owing to a long-term operation and hard-working conditions, the railway clip of a fastening system is exposed to a high risk of relaxing failure[20]. With this in mind, four cases of the metro track were selected differing by the installation of the TRD or not and clips failure. These cases are listed below.

Case I: Metro track without TRD

In Case I, the ideal metro track with no clips' failure is selected and the TRD is not installed. This case is taken as the benchmark for this study.

Case II: Metro track without TRD but clips failure

To consider the clips failure, in Case II the clips at A2 position will be removed from

the fastening system of the test rail, as schematically depicted in Fig. 13.

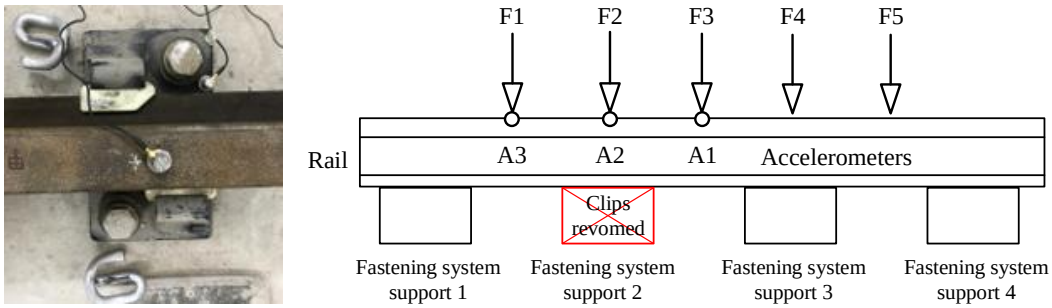

Fig. 13 Track without TRD considering the Disabled Clips at A2

Case III: Metro track with the TRD

In Case III, the ideal metro track is selected and the TRD is installed. A comparative analysis of vibration characteristics of the rail without or with TRD by hammer tests will be carried out.

Case IV: Metro track with TRD but clips failure

Compared with Case III, the clips at A2 position will be removed to form Case IV, and the vibration characteristics of the rail with the TRD considering the disabled clips will be performed. Considering the four test cases described above, the hammer test measurements of metro-tracks were performed in the Rail-Lab. The experimental procedure is described as follows. The light hammer with hard tip was used to hit the excitation locations one by one from F1 to F5, while the recording positions were the same for all the hammer impulses. Then, the output accelerations were transformed into the frequency domain using the Fast Fourier Transform (FFT).

3.1 Typical Vibration Analysis of the 3-interval Rail System

Let us assume Case I (Metro track without TRD) as an example. The time histories of the impulse force from the hammer and the acceleration responses of A1, A2 and A3 for the typical excitation F1 are plotted in Fig. 14, respectively.

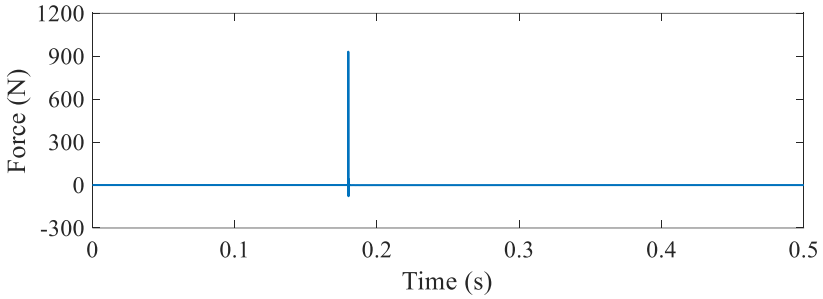

(a) Impulse force

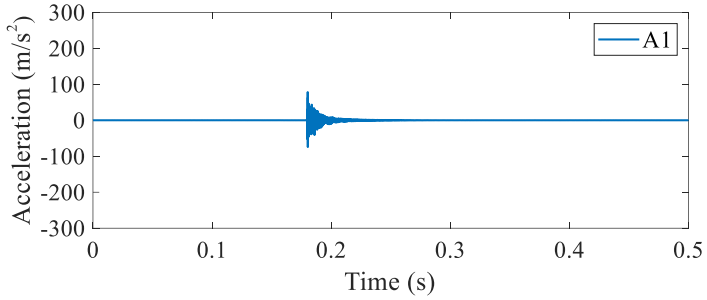

(b) Accelerometer A1

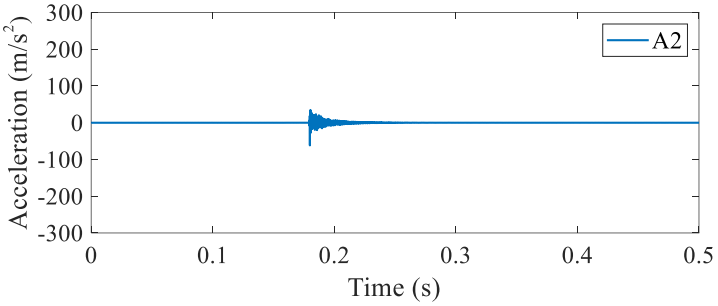

(c) Accelerometer A2

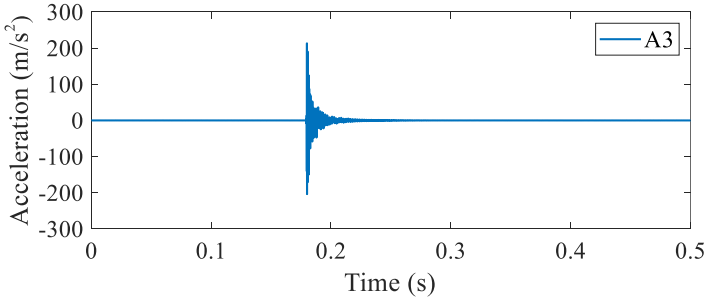

(d) Accelerometer A3

Fig. 14 Typical testing results

As is seen from Fig. 14, the maximum value of the impulse force applied is 931.6 N, and the temporal length of the signals measured is 0.5 s. It was found that the A3 record had larger acceleration values than the others because it is close to the hammer impact

location F1. The acceleration measured at A1 is the median one. Due to the stiff support at the sleepers, the acceleration measured at A2 is much lower than that at A1.

In Case I, the frequencies of an ideal metro track without TRD under the excitations at locations F1, F2, F3, F4 and F5 are shown in Fig.15, respectively. The maximum excitation forces at the five locations from F1 to F5 were 931.6 N, 889.1 N, 982.7 N, 945.8 N and 985.5 N, respectively.

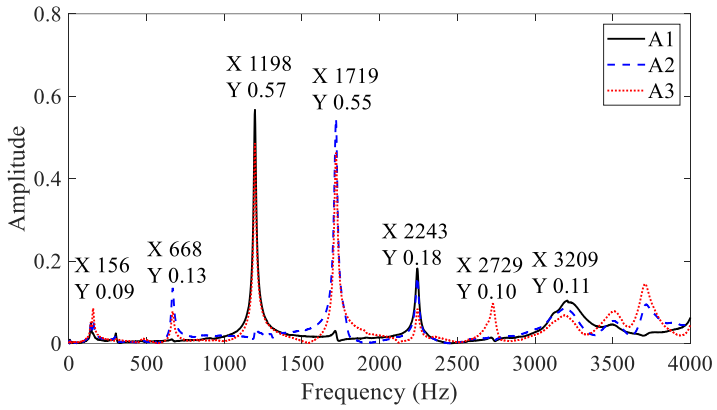

(a) Excitation location F1

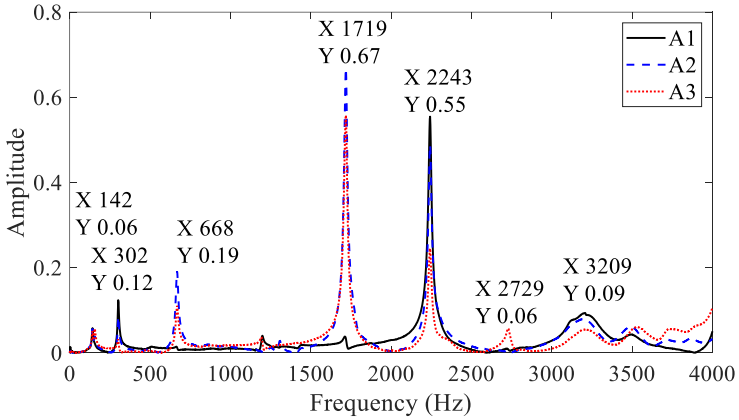

(b) Excitation location F2

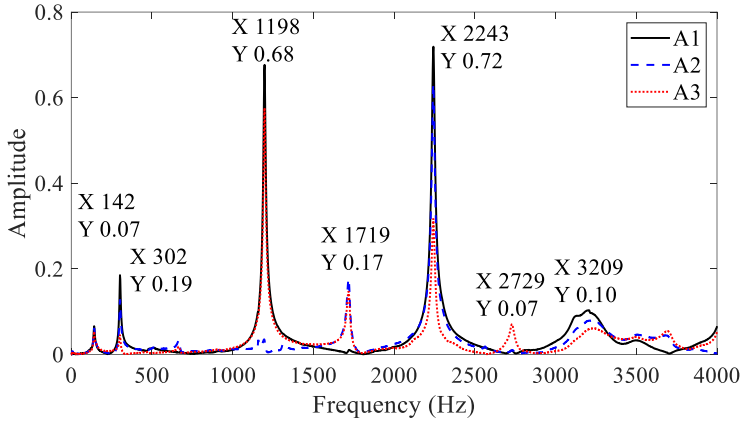

(c) Excitation location F3

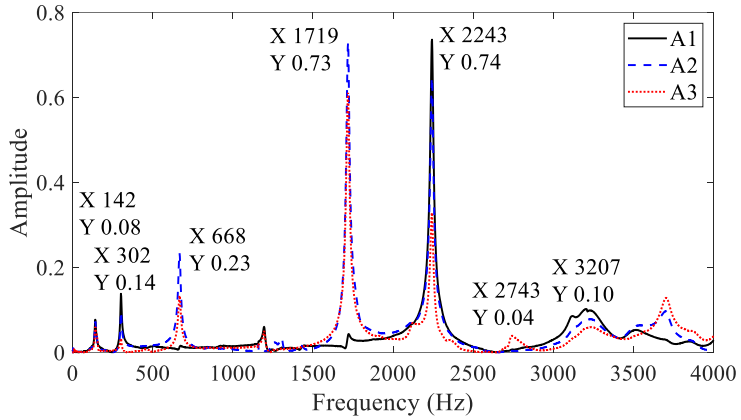

(d) Excitation location F4

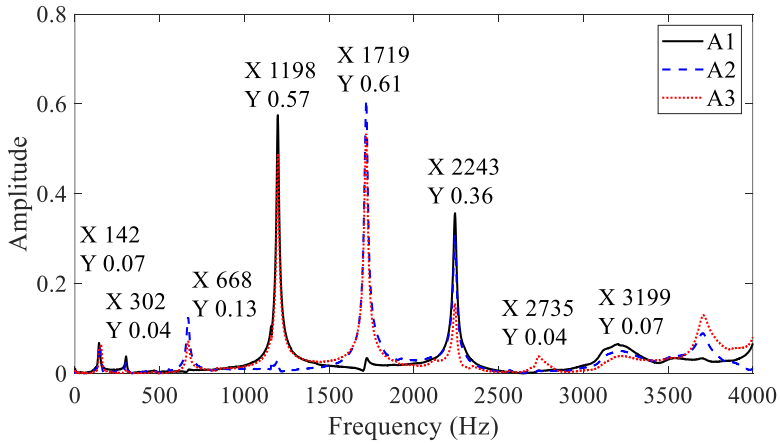

(e) Excitation location F5

Fig. 14 Frequency analysis of the ideal track

It is demonstrated in Fig. 14 that the spectral response curves plotted in Fig. 14(a) are similar to those in Fig. 14(e). Likewise, the response curves shown in Fig. 14(b) are

consistent with those in Fig. 14(d). This is because F1 and F5, as well as F2 and F4 are symmetrically positioned with respect to the center of the rail. As shown in Figs. 14(a) and 14(e), there are two significant response peaks at the frequencies of 1198 Hz and 2243 Hz recorded by the accelerometer A1, three dominant frequencies of 668 Hz, 1719 Hz and 2243 Hz recorded by the accelerometer A2, and all these four peaks were recorded by accelerometer A3.As shown in Figs. 14(b) and 14(d), only one peak at the frequency of 2243 Hz exists on the response curve of accelerometer A1 but three peaks at 668 Hz, 1719 Hz and 2243 Hz are observed from the accelerometers A2 and A3. It is of note that for these two scenarios, the excitation positions F1 and F5 are located at the mid-span sections, while F2 and F4 are positioned at on-support sections. This demonstrates that unexpected frequencies of the test rail are possible to be excited.

3.2 Vibrations of the TRD-Rail Considering the Fastening Effects of Clips

When the TRD was mounted on the metro rail with the clips' failure or without it, the hammer test measurements were performed following the same procedure described in Section 3.1. Let us assume the excitation position at location F3. The spectral response plots resulting from measurements at the metro track representing the Cases I - IV are shown in Table 1. For better comparison, the maximum excitation forces of F3 for Cases I - IV are adjusted as close as possible; they are 1316 N, 1277 N, 1340 N and 1260 N, respectively.

Table 1 Comparison of spectral response of the rails

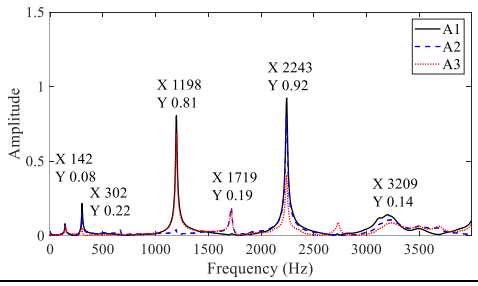	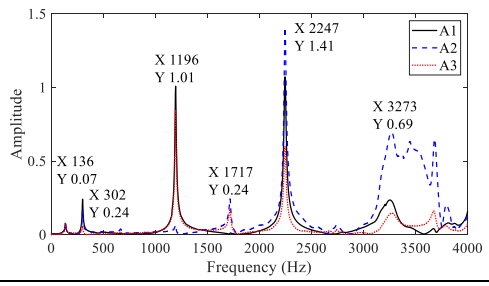
Case I: w/o TRD	Case II: w/o TRD and disabled clips

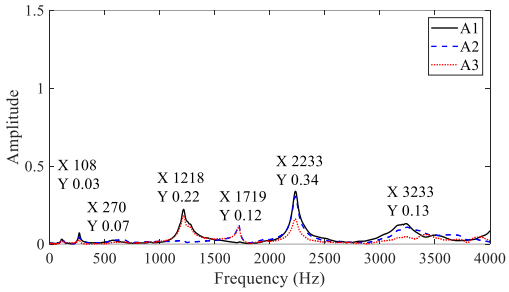	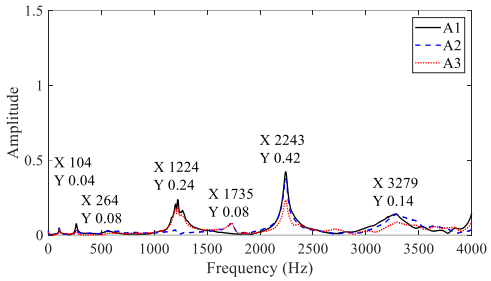
Case III: With TRD	Case IV: With TRD and disabled clips

By comparing the Case I to Case III, it is seen that the interval of frequencies that were excited on the ideal metro track with TRD in high frequency range is slightly shifted to higher values than those of the rail without TRD. For example, the interval from 1198 Hz to 3209 Hz is shifted to 1218 Hz and 3233 Hz, respectively. This can be attributed to the increase of the additional composited flexural stiffness of the TRD-rail combined system, especially in the central part of the rail where the TRDs are mounted on both bottom flange sides of the rail (See Fig. 2(a)). For the lower frequency range, once the TRD is installed on the test rail, the frequency of the ideal track will decrease from 142 Hz to 108 Hz.

In Case III, there are six peaks on the spectral response curves, which correspond to 108 Hz, 270 Hz, 1218 Hz, 1719 Hz, 2233 Hz and 3233 Hz, respectively. In the metro track with the TRDs installed but with disabled clips at A2 (Case IV), the corresponding six peaks change to 104 Hz, 264 Hz, 1224 Hz, 1735 Hz, 2243 Hz and 3279 Hz . This shows that even when the clips are removed from the test track, a small shift of measured frequencies with respect to the track with the TRD still exists. Namely, high frequencies are shifted to higher values and low frequencies to the lower ones. Therefore, the dynamic influence of the disabled clips in a fastening system on the vibration frequencies of the metro track system is rather limited. This is attributed to the fact that the rail-pads above the sleepers can provide enough supporting stiffness to the metro rail. Even when some of the railway clips are removed from the fastening system, the rail-pads still provide sufficient vertical restraints to support the rail.

In these experimental studies, all impulse forces applied to the test rails were kept on the same level. It was found that with the TRD installed on the test track, some of the

response peaks were suppressed in a lower frequency range from 0.92 (or 1.41) to 0.34 (or 0.42). Such a dynamic phenomenon indicates that part of the vibration energy of the rail system has been dissipated or absorbed by the TRD devices. Thus, one can conclude that the TRD has a robust vibration reduction capability to mitigate excessive vibrations of the tracks under repetitive and intensive actions of moving metro trains.

4. Conclusions

To study the dynamic characteristics of a metro track with or without TRD installed, a series of laboratory tests were performed using the prototype of metro tracks in the Rail-Lab of BJTU. The accelerometers were fixed on the top of the rail to collect the response data when the hammer impulses were applied to different excitation positions at locations F1, F2, F3, F4 and F5. Four test cases were selected for analysis and comparison, namely, the ideal track without TRD, the ideal track without TRD but disabled clips, the track with TRD, and the metro track with TRD and disabled clips. The measured acceleration responses were transformed to the frequency domain for detailed spectral response analysis. Some of the interesting findings are summarized as follows: (1) when the hammer impulse forces were applied at different sections, for example, the on-support section or mid-span section, different frequencies of the test rail were excited; (2) the measured frequencies of the rail equipped with the TRD devices slightly increased in higher frequency range when compared to those without TRD; and (3) even when the clips are removed from the fastening system at one supporting sleeper, the proposed TRD can keep its robust vibration reduction capability against intensive vibrations of the metro tracks in operation.

According to the test results of Rail-Lab in BJTU, in addition to convenient installation, the proposed TRD device is a simple, cheap and efficient dynamic absorber that can be mounted, as well as easily replaced on existing metro tracks in operation. Besides, the present laboratory vibration study on metro tracks using the TRDs can be regarded as a preliminary investigation on vibration reduction of a rail system under moving metro cars using passive absorbers. Further theoretical research on the mechanisms of wave attenuation and vibration control for existing rail system using the

proposed TRD absorber needs to be conducted.

Acknowledgments

This study was gratefully sponsored in part by the Fundamental Research Funds for the Central Universities grant number (2022JBMC041), the National Natural Science Foundation of China via grant numbers (52178406), the Portuguese Foundation for Science and Technology (FCT), through IDMEC, under LAETA, project UIDB/50022/2020, the National Science and Technology Council in Taiwan via grant numbers (MOST 110-2221-E-032-008, NSTC 111-2221-E-032-033) and the Taiwan-Czech joint project via grant numbers (MOST 110-2923-E-032-001-MY3, GACR 21-32122J).

Abbreviation

BJTU Beijing Jiaotong University

DTRD Double Tuned Rail Damper

DTVI-2 Ditie fastener type VI-2

SNCF Société Nationale des Chemins de Fer (the French national railway system)

TRD Tuned Rail Damper

References

[1] China Association of Metros (CAMET) (2022) Statistical analysis report on urban rail transit in China 2021. China Metros 10-15.

[2] FENG A (2022) Data Statistics and Development Analysis of Urban Rail Transit in China in 2021. Tunnel Construction 42:336-341.

[3] Zhang H, Liu W, Liu W, Wu Z (2014) Study on the cause and treatment of rail corrugation for Beijing metro. Wear 317:120-128.

[4] Cui X, Huang B, Du Z, Yang H, Jiang G (2020) Study on the Mechanism of the Abnormal Phenomenon of Rail Corrugation in the Curve Interval of a Mountain City Metro. Tribol Trans 63:996-1007.

[5] Wei L, Sun Y, Zeng J, Qu S (2022) Experimental and numerical investigation of fatigue failure for metro bogie cowcatchers due to modal vibration and stress induced by rail corrugation. Eng Fail Anal 142:106810.

[6] Ling L, Li W, Shang H, Xiao X, Wen Z, Jin X (2014) Experimental and numerical investigation of the effect of rail corrugation on the behaviour of rail fastenings. Veh Syst Dyn 52:1211-1231.

[7] Ling L, Li W, Foo E, Wu L, Wen Z, Jin X (2017) Investigation into the vibration of metro bogies induced by rail corrugation. Chin J Mech Eng 30:93-102.

[8] Han J, Xiao X, Wu Y, Wen Z, Zhao G (2018) Effect of rail corrugation on metro interior noise

and its control. Appl Acoust 130:63-70.

[9] Fang G, Wang Y, Peng Z, Wu T (2018) Theoretical investigation into the formation mechanism and mitigation measures of short pitch rail corrugation in resilient tracks of metros. Proc Inst Mech Eng F J Rail Rapid Transit 232:2260-2271.

[10] Li W, Zhou Z, Zhao X, Wen Z, Jin X (2022) Formation mechanism of short-pitch rail corrugation on metro tangent tracks with resilient fasteners. Veh Syst Dyn 1-24.

[11] Grassie S L (2022) The corrugation of railway rails: 1. Introduction and mitigation measures. Proc Inst Mech Eng F J Rail Rapid Transit 1-9.

[12] Maes J, Sol H (2003) A double tuned rail damper-increased damping at the two first pinned-pinned frequencies. J Sound Vib 267:721-737.

[13] Thompson D J, Jones C J C, Waters T P, Farrington D (2007) A tuned damping device for reducing noise from railway track. Appl Acoust 68:43-57.

[14] Chen J, Liu W, Sun X (2017) Effects of Tuned Rail Damper on Track Dynamic Characteristics Optimization. Procedia Engineering 199:1616-1622.

[15] Jin H, Zhou X, Sun X, Li Z (2021) Decay rate of rail with egg fastening system using tuned rail damper. Appl Acoust 172:1-10.

[16] Oregui M, Molodova M, Nunez A, Dollevoet R, Li Z (2015) Experimental Investigation Into the Condition of Insulated Rail Joints by Impact Excitation. Exp Mech 55:1597-1612.

[17] Oregui M, Li Z, Dollevoet R (2015) Identification of characteristic frequencies of damaged railway tracks using field hammer test measurements. Mech Syst Signal Process 54-55:224-242.

[18] Adeagbo M O, Lam H, Chu Y (2022) Bayesian System Identification of Rail-Sleeper-Ballast System in Time and Modal Domains: Comparative Study. ASCE-ASME J Risk Uncertain Eng Syst a Civ Eng 8:4022020.

[19] Alabbasi S, Hussein M, Abdeljaber O, Avci O (2020) A numerical and experimental investigation of a special type of floating-slab tracks. Eng Struct 215:110734.

[20] Ma D, Shi J, Yan Z, Xiao J, Sun L (2022) Experimental and numerical investigation of the effect of the assembled state on the static-dynamic characteristics and fatigue performance of railway fastening clips. Structures 46:1808-1822.